http://dx.doi.org/10.5012/bkcs.2012.33.7.2369

Effect of Al Content on the Gas-Phase Dehydration of Glycerol over Silica-Alumina-Supported Silicotungstic Acid Catalysts

Yong Tae Kim,[a] Su Jin You, Kwang-Deog Jung,[†] and Eun Duck Park[*]

Division of Energy Systems Research and Department of Chemical Engineering, Ajou University, Suwon 443-749, Korea
[*]E-mail: edpark@ajou.ac.kr
[†]Clean Energy Research Center, Korea Institute of Science and Technology, Seoul, Korea
Received February 24, 2012, Accepted April 22, 2012

The gas-phase dehydration of glycerol to acrolein was carried out over silicotungstic acid ($H_4SiW_{12}O_{40}\cdot xH_2O$, HSiW) catalysts supported on SiO_2, η-Al_2O_3, and silica-aluminas with different Al contents. The HSiW catalysts supported on silica-aluminas showed higher glycerol conversions and acrolein yields during the initial 2 h at 315 °C than did SiO_2- and η-Al_2O_3-supported HSiW catalysts. Among the tested catalysts, HSiW/$Si_{0.9}Al_{0.1}O_x$ exhibited the highest space-time yield during the initial 2 h. The loaded HSiW species can change the acid types and suppress the formation of carbonaceous species on Al-rich silica-aluminas. The deactivated HSiW supported on silica-aluminas can be fully regenerated after calcination in air at 500 °C. As long as the molar ratio between water and glycerol was in the range of 2-11, the acrolein selectivity increased significantly with increasing water content in the feed, while the surface carbon content decreased owing to the suppression of heavy compounds.

Key Words : Dehydration, Glycerol, Acrolein, Silica-alumina, Silicotungstic acid

Introduction

The utilization of renewable resources, including biomass, has become an important issue nowadays, because current industrial processes are based on nonrenewable fossil resources (*e.g.*, petroleum, natural gas, and coal) that have limited reservoirs and adverse environmental impacts, including CO_2 accumulation. Glycerol is an important biorefinery feedstock that is available as a byproduct of oleochemistry and can be used to produce valuable chemicals and fuels.[1,2] Glycerol has been oversupplied in this decade as a result of increasing biodiesel production through the transesterification of triglycerides with methanol and ethanol.[1] Among the catalytic routes to glycerol valorization, its dehydration to acrolein is attracting much attention as a replacement for the conventional petroleum-based process in which propylene is selectively oxidized to acrolein over multicomponent Bi-Mo(W)-O based catalysts.[3]

Acrolein is an important key intermediate in acrylic acid production, pharmaceutical production, fiber treatment, and production of other value-added derivatives.[1,2] Several studies have been reported in recent years on solid-acid catalysts such as metal phosphates,[4-7] metal sulfates,[4,8] metal oxides,[4,9-11] supported heteropolyacids (HPAs),[4,12-19] and zeolites[4,20-23] for the dehydration of glycerol to acrolein in the gas phase. Most of these catalysts exhibit superior dehydration activities with higher water/glycerol ratios in the feed at moderate temperatures. However, a catalyst showing a high acrolein yield can easily be deactivated by the strong adsorption of high-molecular-weight organic species and crystalline coke on the strong acid sites in the initial stage of the reaction.[11,22] Several approaches for coping with this catalyst deactivation have been examined, neutralizing undesirable acid sites,[9] decreasing the number of strong acid sites,[16] or changing the porosity[12] in the catalyst. In addition, decreasing the regeneration temperature for the used catalyst without changing the catalyst's structure is an important issue in industrial processes.

In a previous study,[11] we performed the dehydration of glycerol over silica-aluminas with various Si/Al ratios and suggested that silica-aluminas with moderate Brønsted acid sites could be promising candidates for this reaction. Moreover, it was reported that silica-alumina-supported HPAs like silicotungstic acid ($H_4SiW_{12}O_{40}\cdot xH_2O$, HSiW) exhibited outstanding performance and stability.[13,17,18] However, to the best of our knowledge, HPAs supported on silica-aluminas with various Si/Al ratios have not been studied as catalysts for this reaction in detail.

The aim of the present study is to find an optimum Si/Al molar ratio in silica-alumina-supported HSiW catalysts for improving the dehydration activity and decreasing the regeneration temperature. The catalytic activity of η-Al_2O_3- and SiO_2-supported HSiW was also investigated, for comparison. The product distribution as a function of different reaction variables, such as the contact time and the partial pressure of water vapor in the feed, is also presented.

Experimental

Catalyst Preparation. Various supports, *viz*., SiO_2, $Si_{0.98}Al_{0.02}O_x$, $Si_{0.95}Al_{0.05}O_x$, $Si_{0.9}Al_{0.1}O_x$, $Si_{0.8}Al_{0.2}O_x$, $Si_{0.6}Al_{0.4}O_x$,

[a]Present address: Department of Chemical Engineering, University of Massachusetts, Amherst, MA 01003, USA.

$Si_{0.4}Al_{0.6}O_x$, $Si_{0.2}Al_{0.8}O_x$, and η-Al_2O_3, were prepared from $Al(NO_3)\cdot 9H_2O$ (Junsei Chemical Co.) and $Si(OC_2H_5)_4$ (Sigma-Aldrich) according to the method described previously.[11] The precipitates were dried at 60 °C under vacuum for 4 h and further dried at 120 °C overnight, followed by calcination in air at 500 °C for 4 h. Supported HSiW catalysts were prepared from a support and an aqueous solution of HSiW (Alfa Aesar) using a wet impregnation method.[17] The HSiW content was intended to be 15 wt % for all of the supported HSiW catalysts. The HSiW contained about 10 wt % water, which was confirmed using thermogravimetric analysis (TGA) and differential scanning calorimetry (DSC). All of the prepared HSiW catalysts were calcined in air at 400 °C for 4 h and purged in He for 1 h before the reaction.

Characterization of Catalysts. The tungsten contents for all of the prepared catalysts were analyzed using inductively coupled plasma-atomic emission spectroscopy (ICP-AES, JY-70Plus, Jobin-Yvon) and are listed in Table 1.

The Brunauer-Emmett-Teller (BET) surface area was calculated from N_2 physisorption data obtained using a Belsorp mini-II apparatus (BEL JAPAN, Inc.) at liquid N_2 temperature. Before the measurement, the sample was degassed under vacuum for 4 h at 200 °C. The pore volume and average pore diameter for each catalyst were calculated using the Barret-Joyner-Hallender (BJH) desorption method. These data are also presented in Table 1.

The bulk crystalline structures of the catalysts were determined using the X-ray diffraction (XRD) technique. The XRD patterns were obtained with a Rigaku D/MAC-III instrument operated at 50 kV and 30 mA using Cu Kα radiation. The assignment of the crystalline phases was carried out using the PCPDFWIN software (version 2.2) for the ICDD database. The primary crystallite size was measured using Scherrer's equation[24].

After catalyst was saturated with NH_3 at 150 °C for 30 min and flushed with He for 1 h, temperature-programmed desorption of NH_3 (NH_3-TPD) was conducted over 0.10 g of each sample in the temperature range of 150-400 °C at a heating rate of 5 °C/min while the thermal conductivity detector (TCD) signals (AutoChem 2910 unit, Micromeritics) and on-line mass spectrometer signals (QMS 200, Pfeiffer Vacuum) were monitored. All the samples were treated in He at 400 °C before the experiment to remove any adsorbed water or organic species. The peak area can be correlated with the amount of adsorbed NH_3 on the basis of the pulsed NH_3 injection experiment.

After the samples were purged with He at rt for 1 h, temperature-programmed oxidation (TPO) was conducted over 0.05 g of the sample in a 2% O_2/He stream by heating the sample in the temperature range of 30-800 °C at a heating rate of 10 °C/min while monitoring the TCD signals (AutoChem 2910 unit, Micromeritics) and on-line mass spectrometer signals (QMS 200, Pfeiffer Vacuum).

The Raman spectra were recorded on a Nicolet Almega XR Dispersive Raman Spectrometer with a He-Ne 532 nm laser. The laser power was adjusted to ensure that no burning of the catalyst surface occurred.

The amounts of carbon and hydrogen formed on the used catalysts were determined using a CHNS analyzer (Vario EL III) after the samples were pretreated with He at 300 °C to remove any weakly chemisorbed organic compounds before the carbon analysis.

Catalytic Activity Tests[11]**.** The dehydration of glycerol was carried out in a fixed-bed reactor (8 mm in inner diameter and 23.5 cm long) at atmospheric pressure. For the catalyst screening tests, 0.10 g of the catalyst without diluents was loaded into the reactor, and the reactor temperature was increased under He to the final temperature at a heating rate of 4 °C/min. After the catalyst was purged with He at the final temperature for 1 h, it was brought into contact with a reactant gas consisting of 8.3 mol % $C_3H_8O_3$ and 76.3 mol % H_2O in He. A liquid mixture of glycerol and water was fed to the reactor by means of a high-pressure liquid chromatography (HPLC) pump (GILSON 305). The molar flow rate of glycerol, $F_{glycerol}$, was set to 23.4 mmol/h. To examine the effect of the partial pressure of water vapor, we chose the same reaction conditions as those used for the screening tests, except for the molar fraction of water and He in the feed. The molar fraction of glycerol was 8.3 mol % and water/glycerol molar ratios were 2, 9, and 11. The effect of the contact time ($W/F_{glycerol}$) on the catalytic activity was investigated by changing the weight of the catalyst, W, for a fixed feed flow rate (glycerol/water molar ratio = 9).

In all cases, the reactants were preheated to at least 265 °C to prevent partial condensation. The products were collected for analysis in a cold trap maintained at −5 °C at 2 h intervals. They were passed through a 0.2 μm membrane filter and analyzed using gas chromatography (HP-FFAP column with flame ionization detection (FID)). The products were quantified using 1-butanol in water as an external standard.

The glycerol conversion and molar carbon selectivity were quantified according to the following equations:

$$\text{Glycerol conversion (\%)} = \frac{n_{Feed,i} - n_{Feed,o}}{n_{Feed,i}} \times 100$$

$$\text{Molar carbon selectivity (\%)} = \frac{n_{Prod.,o}}{n_{Feed,i} - n_{Feed,o}} \times 100$$

where $n_{Feed,i}$ and $n_{Feed,o}$ are the number of moles of carbon in glycerol at the input and output, respectively, and $n_{Prod.,o}$ is the number of moles of carbon in the product at the output.

Results and Discussion

Table 1 lists the physical properties of the supported HSiW catalysts. Most of the supported HSiW catalysts exhibited less BET surface area, less pore volume, and smaller average pore diameters than did the support itself.[11] The noticeable decrease in the BET surface area and pore volume can likely be ascribed to the plugging of mesopores in the support with the HSiW Keggin structure (Keggin anion diameter ~1.2 nm). The BET surface area increased with increasing molar fractions of Al for supported HSiW

Table 1. Physical properties and NH_3-TPD results for supported HSiW catalysts

Catalyst	W content (wt %)	BET surface area (m^2/g)	Pore volume (cm^3/g)	Average pore diameter (nm)[a]	Total acid amount[b] ($\mu mol\ NH_3/g_{cat.}$)
HSiW/SiO_2	9.6	22	0.15	16.1	42 (0)
HSiW/$Si_{0.95}Al_{0.05}O_x$	8.2	92	0.27	12.1	478 (265)
HSiW/$Si_{0.9}Al_{0.1}O_x$	8.4	110	0.41	15.4	526 (395)
HSiW/$Si_{0.8}Al_{0.2}O_x$	7.1	205	0.51	10.3	423 (425)
HSiW/$Si_{0.6}Al_{0.4}O_x$	8.8	209	0.35	7.0	459 (450)
HSiW/$Si_{0.4}Al_{0.6}O_x$	8.1	229	0.38	6.9	441 (437)
HSiW/$Si_{0.2}Al_{0.8}O_x$	9.1	248	0.41	6.8	408 (384)
HSiW/η-Al_2O_3	9.6	273	0.30	4.7	343 (343)

[a]Average pore diameter was determined using the BJH desorption method. [b]Data in parentheses correspond to the support and were taken from the literature.[10]

catalysts.

To determine the bulk crystalline structure of the supported HSiW catalysts, XRD patterns were obtained for all of them, as shown in Fig. S1 (Supplementary Figure 1). All of the catalysts, except for HSiW/η-Al_2O_3, showed a broad XRD peak with a maximum at $2\theta = 22^o$ attributed to amorphous silica. For the HSiW catalysts supported on Al-rich silica-alumina and η-Al_2O_3, XRD peaks at 2q = 37º, 46º, and 67º attributed to the η-Al_2O_3 (ICDD# 04-0875) phase were found. By comparing the sample XRD patterns with the XRD patterns of each support,[11] it is confirmed that the bulk crystalline structures of the supports did not change during the catalyst preparation. It is worth noting that intense diffraction peaks due to the HSiW (ICDD# 01-0559) phase were observed at 2θ = 11º, 19º, 22º, 24º, and 27º for SiO_2-supported HSiW. These XRD peaks weakened with increasing molar fractions of Al in the supported HSiW catalysts. The presence of strong XRD peaks due to the HSiW phase is related to the poor dispersion of HSiW on supports with low surface areas and low densities of surface anchoring sites for HSiW. Compared with the XRD peaks for HSiW/SiO_2, the diffraction peak at 2θ = 11º representing the (222) plane of HSiW was shifted to a smaller angle for HSiW catalysts supported on silica-aluminas with high Si fractions. Several factors contribute to the increase in the *d*-spacing including changes in the degree of water crystallization[25] and the strong chemical interactions between solids[26] in HPAs. The primary crystalline sizes of HSiW were calculated to be about 3.9, 5.1, and 4.0 nm for HSiW/SiO_2, HSiW/$Si_{0.95}Al_{0.05}O_x$, and HSiW/$Si_{0.9}Al_{0.1}O_x$, respectively, based on Scherrer's equation.

Raman spectra were recorded to identify the nature of the HSiW species on each support, as shown in Figure 1. The SiO_2-supported HSiW showed a strong band at 994 cm^{-1} with a shoulder at 976 cm^{-1} attributed to the symmetric (ν_s) and asymmetric (ν_{as}) W=O stretching modes, respectively.[27] A weak broad band due to the bridging ν(W-O-W) stretching mode appeared at 920 cm^{-1}.[27] The predominant bands were observed at 213 and 154 cm^{-1}, which can be assigned to the ν_s(W-O) stretching mode and d(W-O-W) bending mode, respectively.[27] It is evident that the HSiW Keggin structure is preserved on the silica. Below 300 cm^{-1}, a noticeable loss of spectral intensity in the two predominant

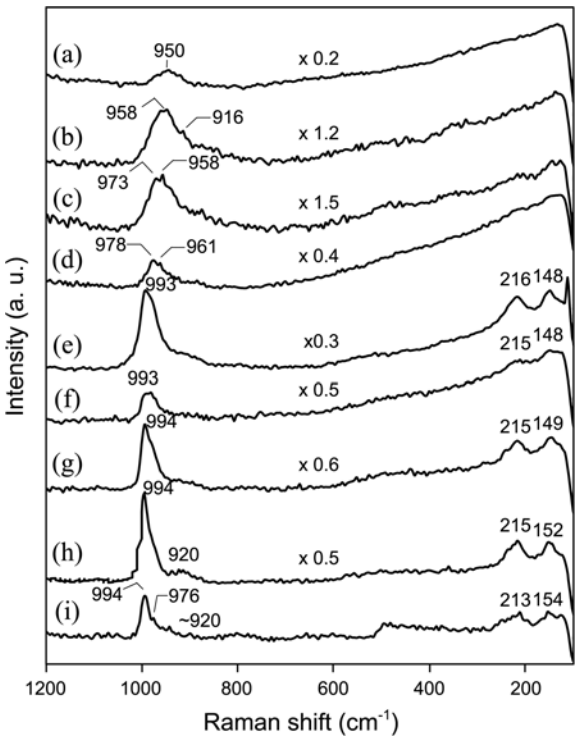

Figure 1. Raman spectra of the supported HSiW catalysts: (a) HSiW/η-Al_2O_3, (b) HSiW/$Si_{0.2}Al_{0.8}O_x$, (c) HSiW/$Si_{0.4}Al_{0.6}O_x$, (d) HSiW/$Si_{0.6}Al_{0.4}O_x$, (e) HSiW/$Si_{0.8}Al_{0.2}O_x$, (f) HSiW/$Si_{0.9}Al_{0.1}O_x$, (g) HSiW/$Si_{0.95}Al_{0.05}O_x$, (h) HSiW/$Si_{0.98}Al_{0.02}O_x$, and (i) HSiW/SiO_2.

bands was observed for HSiW catalysts with molar fractions of Al ranging from 0.4 to 1.0. In the region between 900 and 1000 cm^{-1}, the ν_s(W=O) band was predominant for HSiW catalysts with molar fractions of Al ranging from 0 to 0.2; this result possibly stems from HSiW molecules interacting with themselves.[28] Conversely, a very intense ν_{as}(W=O) mode was observed for HSiW catalysts with molar fractions of Al ranging from 0.4 to 1.0. Moreover, the corresponding band was red-shifted by about 26 cm^{-1} when the molar fraction of Al in the support was increased up to 1.0. This polarizability change in the ν_{as}(W=O) mode likely reflects the loss of electron density in the W=O bond due to distortions in the surface interaction with alumina.[27,28] Although the precise position of the corresponding band is

difficult to determine, there was a broad ν(W-O-W) mode in the catalysts indicating the presence of small amount of polyoxotungstate species.[29] It is confirmed that HSiW strongly interacted with the surface sites of Al_2O_3.

NH_3-TPD was performed to characterize the acidity of the supported HSiW catalysts and the results are shown in Fig. S2 (Supplementary Figure 2). The TPD patterns for all of the prepared catalysts showed a broad peak with a maximum at 212-217 °C and a shoulder at higher temperatures. The total amount of acid sites for the supported HSiW catalysts calculated from the TPD profiles increased when the molar fraction of Al increased up to 0.1 and generally decreased with further increases in the molar fraction of Al, as shown in Table 1. Compared with the total amount of acid sites for the corresponding support,[11] the total acid amount for the supported HSiW catalysts increased with increasing molar fractions of Al in the range from 0 to 0.1. Based on the Raman spectra, it seems that the preservation of the primary HSiW Keggin structure is responsible for an increase in the surface acidity. Caliman *et al.* found that the Brønsted acid sites of the Keggin structure (*e.g.* $H_3PW_{12}O_{40}{\cdot}xH_2O$, HPW) were neutralized by the most basic hydroxyl groups on the alumina surface during the impregnation step.[30] This allows us to speculate why there is no noticeable change in the total acid amount for the other supported HSiW catalysts with molar fractions of Al ranging from 0.4 to 1.0. Namely, it is suggested that the types of acid sites of unsupported HSiW can be changed by the strong interactions between HSiW and Al-rich silica-aluminas.

The dehydration of glycerol was performed over supported HSiW catalysts, and the conversions and yields are presented in Fig. S3 (Supplementary Figure 3) as functions of the time-on-stream. All of the supported HSiW catalysts exhibited higher catalytic activity than did the corresponding support itself.[11] The glycerol conversion and acrolein yield obtained during the initial 2 h increased when the molar fraction of Al in the supported HSiW catalysts increased up to 0.2 and decreased with further increases in the Al molar fraction. HSiW catalysts supported on silica-aluminas showed higher glycerol conversions and acrolein yields during the initial 2 h than did SiO_2- and η-Al_2O_3-supported HSiW catalysts, because the silica-aluminas had higher concentrations of Brønsted acid sites.[11] HSiW/SiO_2 had the lowest dehydration activity because of its low total amount of acid sites.

The product distribution results obtained from the initial 2 h of the dehydration of glycerol over the supported HSiW catalysts are shown in Table 2. The selectivity for acrolein increased linearly with the Al molar fraction up to 0.1 and decreased with further increases in the Al molar fraction. Similarly, the selectivity for acetaldehyde generally increased with increasing in Al molar fractions up to 0.6 and decreased with further increases in the Al molar fraction. The selectivity for side products such as 1-hydroxyacetone, C_1-C_3 alcohols, and C_2-C_3 acids generally increased with the Al molar fraction in the supported HSiW catalysts. The selectivity for unidentified water soluble products, mainly unsaturated hydrocarbons and oxygenates,[6,20] decreased gradually from 25% to 9% with increasing Al molar fractions in the supported HSiW catalysts. Among the tested catalysts, HSiW/$Si_{0.9}Al_{0.1}O_x$ showed the highest acrolein selectivity during the initial 2 h. It is worth mentioning that HSiW/$Si_{0.9}Al_{0.1}O_x$ possessed the largest total amount of acid sites (Table 1). It is also reasonably assumed that most of the

Table 2. Catalytic performance for dehydration of glycerol over supported HSiW catalysts[a,b]

	HSiW/SiO_2	HSiW/ $Si_{0.95}Al_{0.05}O_x$	HSiW/ $Si_{0.9}Al_{0.1}O_x$	HSiW/ $Si_{0.8}Al_{0.2}O_x$	HSiW/ $Si_{0.6}Al_{0.4}O_x$	HSiW/ $Si_{0.4}Al_{0.6}O_x$	HSiW/ $Si_{0.2}Al_{0.8}O_x$	HSiW/ η-Al_2O_3
Conversion (%)	12.1 (2.6)	59.5 (15.1)	65.6 (20.4)	69.9 (18.6)	63.4 (19.5)	60.2 (26.1)	56.4 (30.4)	37.0 (22.7)
Acrolein yield (%)	3.0 (0.9)	24.4 (2.4)	30.1 (4.9)	31.0 (5.5)	27.8 (4.9)	26.0 (9.5)	24.1 (11.7)	12.7 (8.3)
Molar carbon selectivity (%)								
Acrolein	25.0 (33.0)	41.0 (16.2)	46.0 (24.1)	44.4 (29.4)	43.8 (25.2)	43.4 (36.5)	42.6 (38.4)	34.3 (36.4)
Acetaldehyde	0 (0)	1.7 (3.2)	3.2 (5.1)	2.9 (6.0)	3.7 (5.0)	4.2 (5.8)	4.1 (5.4)	2.0 (2.5)
1-Hydroxyacetone	3.3 (3.0)	7.8 (5.7)	8.9 (8.3)	6.3 (6.5)	9.8 (8.5)	9.8 (8.5)	10.1 (11.2)	13.4 (10.7)
Methanol	0.6 (3.0)	0 (0)	0 (0)	0.1 (0.3)	0.1 (0)	0.3 (0.6)	0.5 (0.8)	0.4 (0.3)
Ethanol	0 (0)	0 (0)	0 (0)	0 (0)	0 (0)	0 (0)	0 (0)	0.1 (0)
Allyl alcohol	0 (0)	0.3 (0)	0.4 (0.2)	0.4 (0.4)	0.5 (0.4)	0.7 (0.7)	1.1 (1.1)	1.3 (1.5)
Acetic acid	0.3 (0)	0.8 (0.4)	1.0 (0.4)	0.9 (0.5)	0.9 (0.4)	1.0 (0.6)	1.1 (0.8)	1.1 (0.8)
Propionic acid	0 (0)	0.1 (0)	0.1 (0)	0.1 (0)	0.0 (0)	0.2 (0)	0.2 (0.1)	0.1 (0)
Others	70.9 (61.0)	48.3 (74.6)	40.4 (61.9)	45.0 (57.0)	41.2 (60.5)	40.2 (47.4)	40.3 (42.2)	47.3 (47.9)
Coke deposit[c]								
Carbon content (wt %)	2.5	13.9	17.1	19.2	15.0	16.7	13.8	10.1
H/C	2.6	1.5	1.3	1.2	1.6	1.4	1.6	1.8

[a]Feed composition: 8.3 mol % $C_3H_8O_3$, 76.3 mol % H_2O in He. T = 315 °C, molar flow rate of glycerol = 23.4 mmol/h, weight of the catalyst = 0.10 g, and WHSV = 62 h^{-1}. [b]The conversion, yield, and selectivity were analyzed for the products obtained during the initial 2 h of the reaction. Data in parentheses correspond to the products during the period from 10 to 12 h after the beginning of the reaction. [c]After 12 h of reaction.

acid types on HSiW/$Si_{0.9}Al_{0.1}O_x$ are Brønsted acid sites. Therefore, it can be said that the highest acrolein selectivity over HSiW/$Si_{0.9}Al_{0.1}O_x$ is due to the largest amount of Brønsted acid sites, which is in line with the previous conclusion that the acrolein yield increased with the concentration of the Brønsted acid sites.[11]

In order to examine the effect of the contact time on the space-time yield of acrolein, a long contact time ($W/F_{glycerol}$) of 46.2 $g_{cat.}$·s·$mmol^{-1}$ (*i.e.*, the weight hourly space velocity WHSV = 20.7 h^{-1}) was adopted to monitor the variations in the glycerol conversion and acrolein yield with the time-on-stream, as shown in Fig. S4 (Supplementary Figure 4). The acrolein yield obtained during the initial 2 h increased with increasing molar fractions of Al in the supported HSiW catalysts, reached the maximum value over HSiW/$Si_{0.9}Al_{0.1}O_x$, and then decreased with further increases in the molar fraction of Al in the supported HSiW catalysts. Among the tested catalysts, HSiW/$Si_{0.9}Al_{0.1}O_x$ exhibited the highest space-time yield of acrolein during the initial 2 h, 41.2 mmol/h/g, which is a higher value than that for $Si_{0.8}Al_{0.2}O_x$, 38.6 mmol/h/g.[11]

Table 3 shows the product distribution obtained under the conditions described in Fig. S4. In the case of silica-alumina-supported HSiW catalysts, the glycerol conversion and acrolein selectivity increased as the contact time increased to 41.2 $g_{cat.}$·s·$mmol^{-1}$, but there was a little change in selectivity for side products such as acetaldehyde, 1-hydroxyacetone, C_1-C_3 alcohols, and C_2-C_3 acids. It can be inferred that the formation of 3-hydroxyproionaldehyde (3-HPA), which is an intermediate of acrolein, resulting from mono-dehydration of glycerol, is the rate-determining step for acrolein production over silica-alumina-supported HSiW catalysts. Although the mono-dehydration of glycerol is considered to be the rate-determining step for both acrolein and 1-hydroxyacetone production based on density functional theory (DFT) calculations,[23] the 1-hydroxyacetone produced in this reaction did not change much at different contact times.

Under the reaction conditions used in the present study, the solid acid catalysts did deactivate to a large extent, mainly as a result of the accumulation of carbonaceous species on the Brønsted acid sites, even though the highly concentrated glycerol feedstock is acceptable from a practical viewpoint for producing a high space-time yield of acrolein.[11,17,21,22] Similarly, the glycerol conversion and acrolein yields of all the tested HSiW catalysts also decreased significantly with increasing time-on-stream, as shown in Figs. S3 and S4. On the other hand, the selectivity for side products such as acetaldehyde, 1-hydroxyacetone, C_1-C_3 alcohols, and C_2-C_3 acids did not vary with time-on-stream at either contact time. It is believed that most of the carbonaceous species were deposited on the strong surface acid sites during the initial stage of the reaction, resulting in a loss of accessible active sites due to decreases in the BET surface area and pore diameter.[22]

Tables 2 and 3 present results describing the coke deposit on the used HSiW catalysts obtained using a CHNS analyzer. For the same contact time, the surface carbon content (wt %) of the used catalyst was directly proportional to the acrolein yield obtained during the initial 2 h. There was an increase in the surface carbon content with increasing contact time for the supported HSiW catalysts with Al molar factions of 0.05 and 0.1. On the other hand, no noticeable difference in the surface carbon content was observed for the different contact times for the supported HSiW catalysts

Table 3. Catalytic performance for dehydration of glycerol over supported HSiW catalysts[a,b]

	HSiW/SiO_2	HSiW/ $Si_{0.95}Al_{0.05}O_x$	HSiW/ $Si_{0.9}Al_{0.1}O_x$	HSiW/ $Si_{0.8}Al_{0.2}O_x$	HSiW/ $Si_{0.6}Al_{0.4}O_x$	HSiW/ $Si_{0.4}Al_{0.6}O_x$	HSiW/ $Si_{0.2}Al_{0.8}O_x$	HSiW/ η-Al_2O_3
Conversion (%)	23.3 (3.5)	95.0 (32.9)	97.2 (42.6)	95.5 (43.4)	93.7 (37.4)	90.3 (51.0)	79.4 (56.9)	86.9 (57.0)
Acrolein yield (%)	5.6 (0.5)	47.6 (9.4)	52.8 (14.3)	48.3 (14.8)	47.4 (11.6)	42.5 (18.8)	37.2 (21.2)	29.1 (21.9)
Molar carbon selectivity (%)								
Acrolein	24.0 (13.6)	50.1 (28.5)	54.4 (33.3)	50.6 (34.1)	50.1 (31.2)	47.0 (36.4)	46.8 (37.3)	33.5 (38.5)
Acetaldehyde	0.3 (0)	3.1 (4.0)	4.4 (5.0)	5.8 (6.1)	4.5 (4.7)	5.7 (5.8)	4.9 (5.1)	2.4 (2.4)
1-Hydroxyacetone	6.1 (4.2)	8.3 (9.5)	8.9 (10.9)	9.1 (12.3)	8.7 (11.1)	10.9 (14.1)	12.3 (13.2)	13.4 (18.7)
Methanol	0 (0)	0 (0)	0 (0.1)	0 (0.2)	0.2 (0.3)	0.4 (0.7)	0.7 (1.1)	0.5 (0.7)
Ethanol	0 (0)	0 (0)	0 (0)	0 (0)	0 (0)	0.1 (0.1)	0.1 (0.2)	0.1 (0.1)
Allyl alcohol	0.5 (0)	0.4 (0.3)	0.5 (0.4)	0.5 (0.4)	0.6 (0.5)	0.8 (0.8)	1.4 (1.4)	1.3 (1.8)
Acetic acid	0.4 (1.8)	1.0 (0.7)	1.0 (0.5)	0.9 (0.6)	0.7 (0.5)	0.9 (0.7)	0.9 (0.8)	1.0 (1.0)
Propionic acid	0 (0)	0.2 (0.1)	0.3 (0.1)	0.3 (0.1)	0.2 (0.1)	0.3 (0.2)	0.3 (0.2)	0.2 (0.1)
Others	68.7 (80.5)	36.9 (56.8)	30.6 (49.6)	32.8 (46.2)	34.9 (51.7)	33.9 (41.2)	32.5 (40.8)	47.6 (36.3)
Coke deposit[c]								
Carbon content (wt %)	2.5	15.8	19.6	19.1	15.5	15.7	12.8	10.8
H/C	4.0	1.3	1.2	1.3	1.6	1.6	1.8	1.8

[a]Feed composition: 8.3 mol % $C_3H_8O_3$, 76.3 mol % H_2O in He. T = 315 °C, molar flow rate of glycerol = 23.4 mmol/h, weight of the catalyst = 0.30 g, and WHSV = 20.7 h^{-1}. [b]The conversion, yield, and selectivity were analyzed for the products obtained during the initial 2 h of the reaction. Data in parentheses correspond to the products during the period from 10 to 12 h after the beginning of the reaction. [c]After 12 h of reaction.

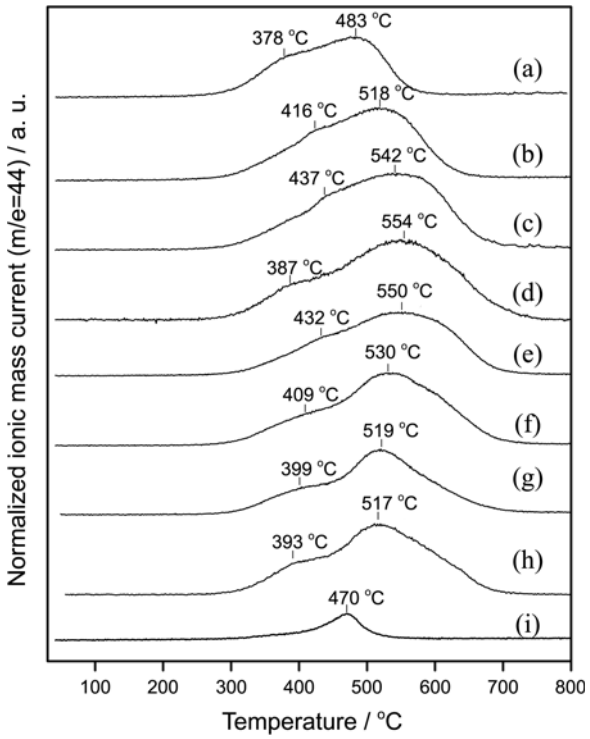

Figure 2. Temperature-programmed oxidation (TPO) patterns of the supported HSiW catalysts after the glycerol dehydration reaction: (a) η-Al_2O_3, (b) $Si_{0.2}Al_{0.8}O_x$, (c) $Si_{0.4}Al_{0.6}O_x$, (d) $Si_{0.6}Al_{0.4}O_x$, (e) $Si_{0.8}Al_{0.2}O_x$, (f) $Si_{0.9}Al_{0.1}O_x$, (g) $Si_{0.95}Al_{0.05}O_x$, (h) $Si_{0.98}Al_{0.02}O_x$, and (i) SiO_2. Feed composition: 8.3 mol % $C_3H_8O_3$, 76.3 mol % H_2O in He. *T*: 315 °C. Molar flow rate of glycerol: 23.4 mmol/h. The weight of the catalyst was 0.30 g; WHSV = 20.7 h^{-1}.

with Al molar fractions ranging from 0.2 to 1.0. In the case of the used HSiW/SiO_2, the surface carbon content was the lowest among the tested catalysts and did not change with the contact time.

TPO was performed to characterize the surface carbon species deposited on the supported HSiW catalysts after 12 h of the reaction, and the results are depicted in Figure 2. Distinguishable TPO peaks representing carbon dioxide (*m/e* = 44) were observed in medium- and high-temperature regions over the tested HSiW catalysts. For SiO_2- and η-Al_2O_3-supported HSiW catalysts, maximum TPO peaks centered at about 470 and 483 °C, respectively, were observed, and these could be mainly attributed to the carbon species formed on HSiW on each support. The appearance of these TPO peaks implies that the surface carbon species deposited on HSiW on SiO_2 and η-Al_2O_3 can be more easily oxidized to carbon dioxide at lower temperatures than the more strongly bound deposits on the HSiW supported on silica-aluminas. Moreover, the maximum peaks were at lower temperatures for HSiW catalysts supported on silica-alumina than for the corresponding support.[11] This implies that the strong interaction between carbon species and surface acid sites can be weakened when HSiW is introduced onto silica-aluminas. The catalytic activity was measured after a regeneration step in which the deposited carbonaceous species were burned off in an air stream at a relatively low temperature, and the results are shown in Figure 3. The more coke can be removed with increasing regeneration temperature but the Keggin structure can be destroyed at high temperatures. Therefore, the proper regeneration temperature was selected not only to maximize the coke removal but also to minimize the destruction of Keggin structure of supported HSiW catalysts. When $Si_{0.9}Al_{0.1}O_x$- and $Si_{0.4}Al_{0.6}O_x$-supported HSiW catalysts were calcined in air at 500 °C after 12 h of reaction, the surface carbon contents decreased to 2.2 and 2.0 wt %, respectively. The H/C ratios were also determined to be 4.0 and 7.4, respectively. This implies that most of the surface carbon was removed, and the remaining carbon species had a much higher H/C ratio than those of the corresponding used catalysts before the regeneration step.

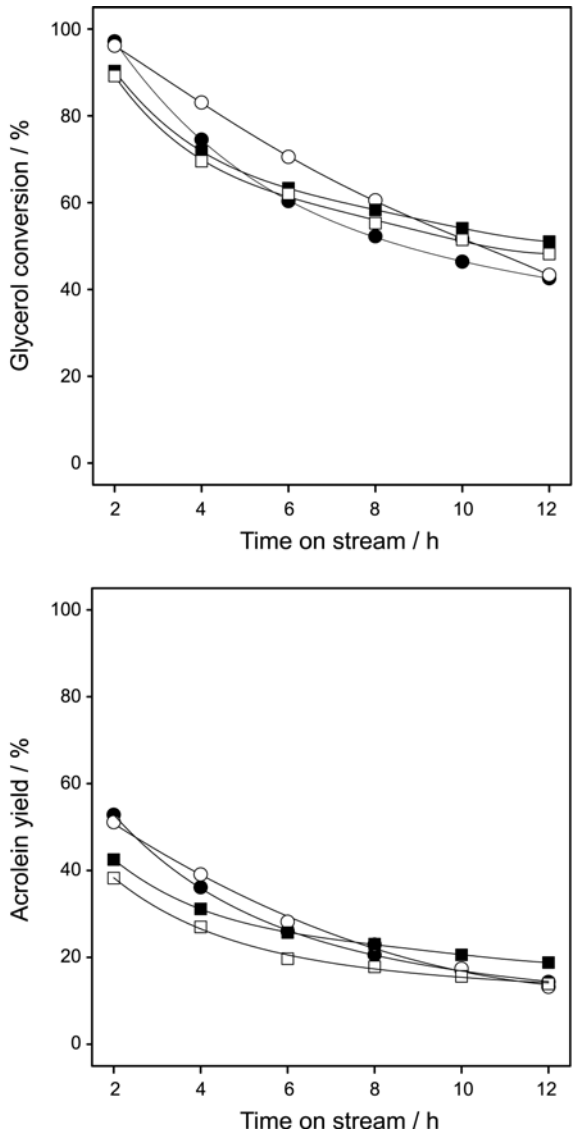

Figure 3. Variations in glycerol conversion and acrolein yield with time-on-stream over the supported HSiW catalysts: fresh HSiW/$Si_{0.9}Al_{0.1}O_x$ (●), fresh HSiW/$Si_{0.4}Al_{0.6}O_x$ (■), HSiW/$Si_{0.9}Al_{0.1}O_x$ regenerated in air at 500 °C (○), and HSiW/$Si_{0.4}Al_{0.6}O_x$ regenerated in air at 500 °C (□). Feed composition: 8.3 mol % $C_3H_8O_3$, 76.3 mol % H_2O in He. *T*: 315 °C. Molar flow rate of glycerol: 23.4 mmol/h. The weight of the catalyst was 0.30 g; WHSV = 20.7 h^{-1}.

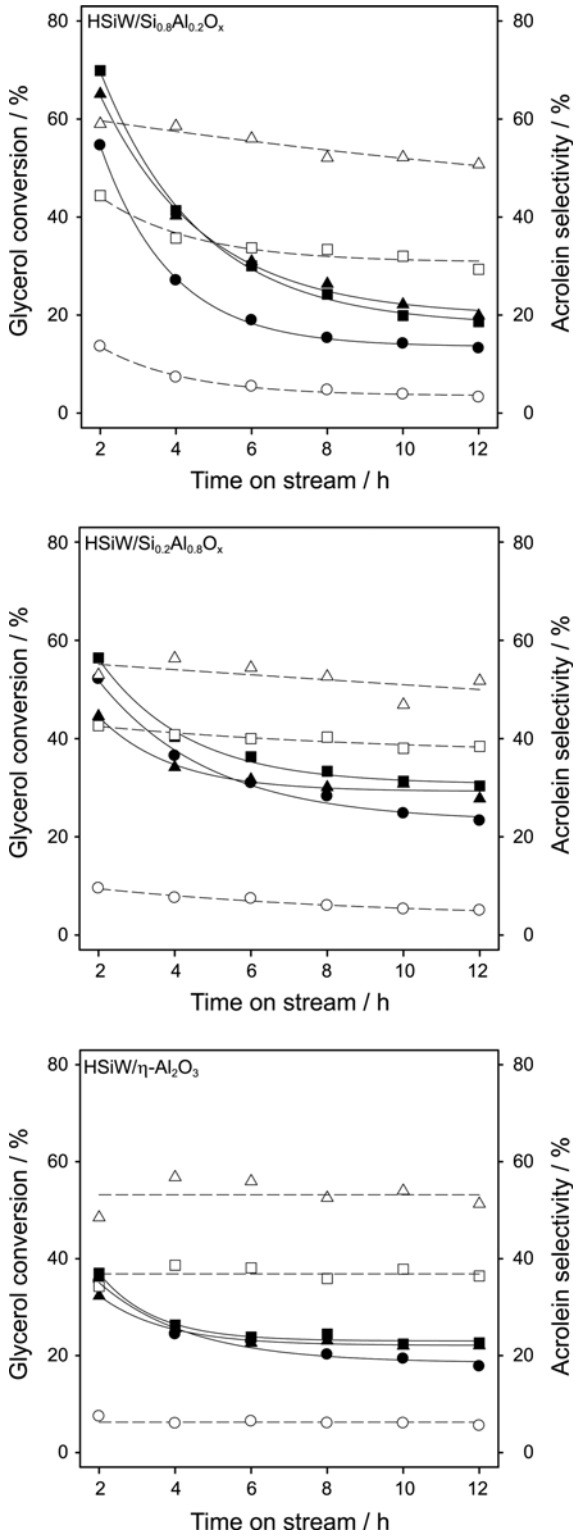

Figure 4. Variations in glycerol conversion (closed symbols) and acrolein selectivity (open symbols) over HSiW/Si$_{0.8}$Al$_{0.2}$O$_x$, HSiW/Si$_{0.2}$Al$_{0.8}$O$_x$, and HSiW/η-Al$_2$O$_3$ with time-on-stream at different water content in the feed. Feed compositions: 8.3 mol % $C_3H_8O_3$ and (●, ○) 15.7, (■, □) 76.3, and (▲, △) 91.7 mol % H_2O in He. *T*: 315 °C. Molar flow rate of glycerol: 23.4 mmol/h. The weight of the catalyst was 0.10 g; WHSV = 62 h^{-1}.

As shown in Figure 3, the regenerated catalysts exhibited glycerol conversions and acrolein yields similar to those of the fresh catalyst. This result implies that these catalysts can be used in the continuous flow reaction system with a regenerative cycle, which is very important from the practical point of view because the coke-resistant catalyst has not been developed for this reaction. In order to find out any change in the structures of HSiW species during the regeneration step, Raman spectra were obtained for HSiW/Si$_{0.4}$Al$_{0.6}$O$_x$ and HSiW/Si$_{0.9}$Al$_{0.1}$O$_x$ both regenerated in air 500 °C and were compared with those of fresh catalyst calcined in air at 400 °C (Figure S5). In the case of HSiW/Si$_{0.4}$Al$_{0.6}$O$_x$ catalysts, there was no distinguishable difference in Raman spectra between them, which implies that the initial structure was preserved even after a regeneration step. On the other hand, the HSiW/Si$_{0.9}$Al$_{0.1}$O$_x$ catalyst regenerated in air at 500 °C exhibited two strong bands at 808 and 720 cm^{-1} representing the stretching and bending modes of WO_3.[29] Therefore, it can be said that the Keggin structure in HSiW/Si$_{0.9}$Al$_{0.1}$O$_x$ was destroyed during the regeneration step.

The dehydration of glycerol was performed with different water contents in the feed over Si$_{0.8}$Al$_{0.2}$O$_x$-, Si$_{0.2}$Al$_{0.8}$O$_x$-, and η-Al$_2$O$_3$-supported HSiW catalysts, and the results are depicted in Figure 4. For all experiments, the glycerol concentration in the feed was fixed to 8.3 mol %. For Si$_{0.8}$Al$_{0.2}$O$_x$-supported HSiW catalysts, the glycerol conversion obtained during the initial 2 h increased when the water content in the feed increased from 15.7% to 76.3% and did not increase further with further increases in the water content in the feed to 91.7%. On the other hand, for η-Al$_2$O$_3$-supported HSiW catalysts, no noticeable change was found in the glycerol conversion obtained during the initial 2 h. In all cases, the selectivity for acrolein obtained during the initial 2 h significantly increased with increasing water content in the feed. As can be seen from Table 4, the selectivity for acetaldehyde also increased with an increase in the water content in the feed, whereas the selectivity for 1-hydroxyacetone, C_1-C_3 alcohols, and C_2-C_3 acids did not vary with the water content in the feed. Notably, the selectivity for water-insoluble heavy compounds, mainly formed by condensation reactions between reactive products such as acrolein, significantly decreased with increasing water content in the feed (data not shown). This is practically important because the suppression of heavy compounds resulting from an increase in the water content in the feed is accompanied by a decrease in the surface carbon species deposited on the strong acid sites.

Conclusion

HSiW supported on silica-aluminas showed a higher glycerol conversion and acrolein yield during the initial 2 h at 315 °C than did SiO$_2$- and η-Al$_2$O$_3$-supported HSiW. Among the tested catalysts, HSiW/Si$_{0.9}$Al$_{0.1}$O$_x$ exhibited the highest space-time yield during the initial 2 h. All of the supported HSiW catalysts exhibited higher catalytic activities than did the corresponding supports themselves. The introduced HSiW can change the type of acid sites and suppress

Table 4. Catalytic performance for dehydration of glycerol for various water contents in the feed over supported HSiW catalysts[a,b]

	HSiW/$Si_{0.8}Al_{0.2}O_x$	HSiW/$Si_{0.8}Al_{0.2}O_x$	HSiW/$Si_{0.2}Al_{0.8}O_x$	HSiW/$Si_{0.2}Al_{0.8}O_x$	HSiW/η-Al_2O_3	HSiW/η-Al_2O_3
Water content in a feed (mol %)	15.7	91.7	15.7	91.7	15.7	91.7
Conversion (%)	54.6 (13.2)	65.1 (19.9)	52.1 (23.3)	44.6 (27.8)	35.3 (17.8)	32.3 (22.1)
Acrolein yield (%)	7.4 (0.4)	38.4 (10.1)	5.0 (1.2)	23.6 (14.4)	2.6 (1.0)	15.7 (11.3)
Molar carbon selectivity (%)						
Acrolein	13.6 (3.2)	59.0 (50.8)	9.5 (5.0)	53.0 (51.8)	7.5 (5.6)	48.5 (51.3)
Acetaldehyde	2.2 (3.6)	5.8 (10.5)	3.0 (3.5)	6.2 (7.9)	1.8 (2.0)	3.2 (3.7)
1-Hydroxyacetone	10.9 (12.7)	9.3 (11.5)	14.1 (18.8)	14.5 (15.6)	16.1 (22.4)	17.6 (17.4)
Methanol	0.3 (1.0)	0 (0)	0.4 (1.2)	0.3 (0.6)	0.5 (0.6)	0.1 (0.2)
Ethanol	0 (0)	0 (0)	0.1 (0.1)	0 (0)	0 (0)	0 (0)
Allyl alcohol	0.6 (0.6)	0.4 (0.4)	0.8 (1.1)	0.9 (1.0)	0.9 (1.1)	1.1 (1.2)
Acetic acid	1.2 (0.5)	1.0 (0.7)	1.3 (0.5)	1.0 (0.7)	1.3 (0.7)	1.1 (0.7)
Propionic acid	0 (0)	0.1 (0)	0.2 (0)	0.2 (0)	0.1 (0)	0 (0)
Others	71.2 (78.5)	24.3 (26.2)	70.6 (69.7)	23.9 (22.5)	71.8 (67.7)	28.5 (25.5)
Coke deposit[c]						
Carbon content (wt %)	21.2	15.6	17.8	13.2	12.5	10.2
H/C	1.3	1.5	1.6	1.9	1.9	2.2

[a]Feed composition: 8.3 mol % $C_3H_8O_3$, and 15.7 or 91.7 mol % H_2O in He. T = 315 °C, molar flow rate of glycerol = 23.4 mmol/h, weight of the catalyst = 0.10 g, and WHSV = 62 h^{-1}. [b]The conversion, yield, and selectivity were analyzed for the products obtained during the initial 2 h of the reaction. Data in parentheses correspond to the products during the period from 10 to 12 h after the beginning of the reaction. [c]After 12 h of reaction.

the formation of carbonaceous species on silica-aluminas. The deactivated HSiW supported on silica-aluminas can be fully regenerated after calcination in air at 500 °C. As long as the molar ratio between water and glycerol was in the range of 2-11, the selectivity for acrolein significantly increased with increasing water content of the feed, while the surface carbon content decreased owing to the suppression of heavy compounds.

Acknowledgments. This research was supported by the Priority Research Centers Program through the National Research Foundation of Korea (NRF) funded by the Ministry of Education, Science and Technology (2010-0029617). In addition, this work was financially supported by a grant from the Industrial Source Technology Development Programs (10033099) of the Ministry of Knowledge Economy (MKE) of Korea. Dr. Kwang-Deog Jung appreciates the financial support by the Korea Government Ministry of Knowledge Economy, Converging Research Center Program (2011K000660) through the National Research Foundation of Korea (NRF) and the Ministry of Education, Science and Technology.

Supporting Information. All supplementary Figures 1-4 are available *via* the Internet, http://newjournal.kcsnet.or.kr.

References

1. Zheng, Y.; Chen, X.; Shen, Y. *Chem. Rev.* **2008**, *108*, 5253.
2. Katryniok, B.; Paul, S.; Bellière-Baca, V.; Rey, P.; Dumeignil, F. *Green Chem.* **2010**, *12*, 2079.
3. Bettahar, M. M.; Costentin, G.; Savary, L.; Lavalley, J. C. *Appl. Catal. A: Gen.* **1996**, *145*, 1.
4. Chai, S.-H.; Wang, H.-P.; Liang, Y.; Xu, B.-Q. *Green Chem.* **2007**, *9*, 1130.
5. Wang, F.; Dubois, J.-L.; Ueda, W. *J. Catal.* **2009**, *268*, 260.
6. Suprun, W.; Lutecki, M.; Haber, T.; Papp, H. *J. Mol. Catal. A: Chem.* **2009**, *309*, 71.
7. Suprun, W.; Lutecki, M.; Gläser, R.; Papp, H. *J. Mol. Catal. A: Chem.* **2011**, *342-343*, 91.
8. Cavani, F.; Guidetti, S.; Marinelli, L.; Piccinini, M.; Ghedini, E.; Signoretto, M. *Appl. Catal. B: Environ.* **2010**, *100*, 197.
9. Lauriol-Garbay, P.; Millet, J. M. M.; Loridant, S.; Bellière-Baca, V.; Rey, P. *J. Catal.* **2011**, *280*, 68.
10. Ulgen, A.; Hoelderich, W. F. *Appl. Catal. A: Gen.* **2011**, *400*, 34.
11. Kim, Y. T.; Jung, K.-D.; Park, E. D. *Appl. Catal. B: Environ.* **2011**, *107*, 177.
12. Tsukuda, E.; Sato, S.; Takahashi, R.; Sodesawa, T. *Catal. Commun.* **2007**, *8*, 1349.
13. Atia, H.; Armbruster, U.; Martin, A. *J. Catal.* **2008**, *258*, 71.
14. Chai, S.-H.; Wang, H.-P.; Liang, Y.; Xu, B.-Q. *Green Chem.* **2008**, *10*, 1087.
15. Alhanash, A.; Kozhevnikova, E. F.; Kozhevnikov, I. V. *Appl. Catal. A: Gen.* **2010**, *378*, 11.
16. Katryniok, B.; Paul, S.; Capron, M.; Lancelot, C.; Bellière-Baca, V.; Rey, P.; Dumeignil, F. *Green Chem.* **2010**, *12*, 1922.
17. Kim, Y. T.; Jung, K.-D.; Park, E. D. *Bull. Korean Chem. Soc.* **2010**, *31*, 3283.
18. Atia, H.; Armbruster, U.; Martin, A. *Appl. Catal. A: Gen.* **2011**, *393*, 331.
19. Erfle, S.; Armbruster, U.; Bentrup, U.; Martin, A.; Brückner, A. *Appl. Catal. A: Gen.* **2011**, *391*, 102.
20. Corma, A.; Huber, G. W.; Sauvanaud, L.; O'Connor, P. *J. Catal.* **2008**, *257*, 163.
21. Kim, Y. T.; Jung, K.-D.; Park, E. D. *Micropor. Mesopor. Mat.* **2010**, *131*, 28.
22. Kim, Y. T.; Jung, K.-D.; Park, E. D. *Appl. Catal. A: Gen.* **2011**, *393*, 275.
23. Kongpatpanich, K.; Nanok, T.; Boekfa, B.; Probst, M.; Limtrakul, J. *Phys. Chem. Chem. Phys.* **2011**, *13*, 6462.
24. Kim, Y. T.; Park, E. D. *Korean J. Chem. Eng.* **2010**, *27*, 1123.
25. Mioè, U.B.; Dimitrijeviæ, R. Ž.; Davidoviæ, M.; Nediæ, Z. P.;

Mitroviæ, M. M.; Colomban, P. H. *J. Mater. Sci.* **1994**, *29*, 3705.
26. Dias, J. A.; Caliman, E.; Dias, S. C. L.; Paulo, M.; de Souza, A. T. C. P. *Catal. Today* **2003**, *85*, 39.
27. Teague, C. M.; Li, X.; Biggin, M. E.; Lee, L.; Kim, J.; Gewirth, A. A. *J. Phys. Chem. B* **2004**, *108*, 1974.
28. Formo, E. V.; Wu, Z.; Mahurin, S. M.; Dai, S. *J. Phys. Chem. C* **2011**, *115*, 9068.
29. Scheithauer, M.; Grasselli, R. K.; Knözinger, H. *Langmuir* **1998**, *14*, 3019.
30. Caliman, E.; Dias, J. A.; Dias, S. C. L.; Prado, A. G. S. *Catal. Today* **2005**, *107-108*, 816.